

## Gibbs-Thomson formula for small island sizes: Corrections for high vapor densities

Badrinarayan Krishnamachari, James McLean,\* Barbara Cooper, and James Sethna  
*Laboratory of Atomic and Solid State Physics, Cornell University, Ithaca, New York 14853*

(Received 1 April 1996)

In this paper we report simulation studies of equilibrium features, namely, circular islands on model surfaces, using Monte Carlo methods. In particular, we are interested in studying the relationship between the density of vapor around a curved island and its curvature. The ‘‘classical’’ form of this relationship is the Gibbs-Thomson formula, which assumes that the vapor surrounding the island is an ideal gas. Numerical simulations of a lattice gas model, performed for various sizes of islands, do not fit very well to the Gibbs-Thomson formula. We show how corrections to this form arise at high vapor densities, wherein a knowledge of the exact equation of state (as opposed to the ideal-gas approximation) is necessary to predict this relationship. By exploiting a mapping of the lattice gas to the Ising model, one can compute the corrections to the Gibbs-Thomson formula using high field series expansions. The corrected Gibbs-Thomson formula matches very well with the Monte Carlo data. We also investigate finite size effects on the stability of the islands both theoretically and through simulations. Finally, the simulations are used to study the microscopic origins of the Gibbs-Thomson formula. It is found that smaller islands have a greater adatom detachment rate per unit length of island perimeter. This is principally due to a lower coordination of edge atoms and a greater availability of detachment moves relative to edge moves. A heuristic argument is suggested in which these effects are partially attributed to geometric constraints on the island edge. [S0163-1829(96)01635-9]

### I. INTRODUCTION

The study of the stability and evolution of nanoscale features is useful in understanding microscopic processes involved in the formation and growth of solids. Theoretical studies of the coarsening of an ensemble of ‘‘islands’’<sup>1</sup> as well as models for the decay of single nanoscale ‘‘islands,’’<sup>2-4</sup> make use of the fact that there exists a high vapor pressure in equilibrium with extremely small islands on the surface. These theories which describe systems away from equilibrium make use of the relationship between the equilibrium vapor pressure around a circular island and the curvature of the island, which is given by the Gibbs-Thomson formula. In this paper, we shall take a closer look at this formula and show that it needs important corrections at high vapor densities wherein interaction between atoms of the vapor cannot be ignored. We will discuss the two-dimensional problem of an island in equilibrium with a vapor of adatoms on the surrounding terrace. We will ignore the (often small) three-dimensional bulk evaporation-condensation and bulk vapor pressure.

For a two-dimensional island of radius  $r$  in equilibrium with the vapor of adatoms around it, the Gibbs-Thomson formula<sup>5,6</sup> is

$$p(r) = p_{\infty} \exp[\gamma / (r \rho_s k_B T)], \quad (1)$$

where  $p_{\infty}$  is the vapor pressure outside a straight interface between solid and vapor,  $\gamma$  is the edge free energy per unit length of the two-dimensional island on the substrate,  $\rho_s$  is the density of the solid island,  $k_B$  is Boltzmann’s constant, and  $T$  the absolute temperature. This relation assumes that the gas surrounding an island is ‘‘ideal’’ and hence we may write down a similar expression for the density of the gas in equilibrium with an island of radius  $r$  as

$$\rho(r) = \rho_{\infty} \exp[\gamma / (r \rho_s k_B T)]. \quad (2)$$

The above equation is often seen in the context of nucleation theory of growth in first order phase transformations<sup>5</sup> in addition to its application to the study of equilibrium and decay of features on surfaces.

Section II discusses the derivation of the ‘‘classical’’ Gibbs-Thomson formula for a finite size system having a constant number of atoms. We simulate a two-dimensional lattice gas on a square lattice, using Monte Carlo techniques, in order to test this relation and find that the Gibbs-Thomson formula deviates significantly from the data from our simulation (Sec. III). This is because of the assumption that the vapor around the island is an ideal gas. In our case, we can map the lattice gas to the Ising model, enabling us to use high field series expansions to generate an equation of state for the lattice gas that improves upon the ideal-gas assumption. This is used to derive a corrected Gibbs-Thomson formula in Sec. IV. This corrected Gibbs-Thomson formula gives a very good description of the data obtained from the simulation. In Sec. V we discuss the constraint of finite size along with predictions regarding the stability of the islands. We investigate the microscopic origins of the enhanced vapor pressure around small islands in Sec. VI and present a plausible argument in which we try to correlate the enhancement with geometric constraints on the island. We finally conclude with Sec. VII.

### II. THE GIBBS-THOMSON FORMULA

The Gibbs-Thomson formula is encountered frequently in the study of curved interfaces in equilibrium.<sup>6</sup> It is also en-

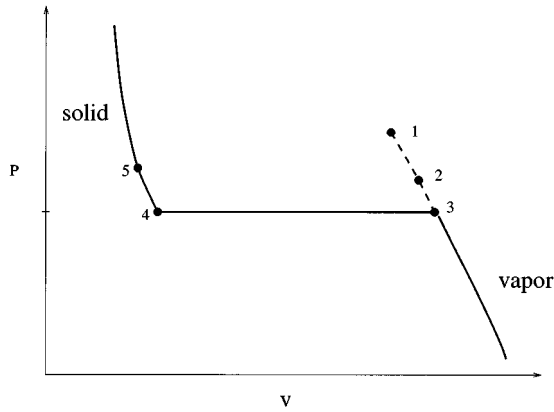


FIG. 1. Equation of state for the ideal gas.

countered in the context of nucleation and critical droplet theory (for first order phase transformations),<sup>5</sup> wherein one studies the formation of droplets of liquid (analogous to the solid islands mentioned in the introduction) in a supersaturated gas and the free-energy barrier to the formation of these droplets. However, in this context, the droplet formed is often at a saddle point of the total free energy of the system, in short an unstable, stationary state. These droplets can be stabilized by finite size effects.<sup>7</sup> If the system under study (with a fixed number of atoms) is placed in a box of fixed volume and temperature then one can show that under certain conditions the global minimum of the free energy of the system consists of a droplet/island in equilibrium with its vapor and the relationship between the island size and vapor pressure is given by the Gibbs-Thomson formula.

We will now derive the Gibbs-Thomson formula for this system. Consider  $N$  atoms of supersaturated vapor in a two-dimensional box of volume  $V$ , at a temperature  $T$ . The system is at a metastable state on its phase diagram (point 1 in Fig. 1), because the supersaturated vapor can lower its Helmholtz free energy by nucleating a solid island (point 5 on the phase diagram), which would be in equilibrium with the remaining vapor around it (point 2)<sup>8</sup>. We will show this explicitly by computing the change in free energy of the system upon nucleation of an island.

The change in Helmholtz free energy of the system on nucleating a solid island of radius  $r$ , from the supersaturated vapor, has three pieces to it:

(a) An increase in edge free energy of the island formed given by

$$\Delta F_{\text{edge}} = 2\pi r\gamma, \quad (3)$$

where  $\gamma$  is the line tension or free energy per unit length of the edge.

(b) A change in the bulk free energy of the condensing atoms. If the number density of the solid formed is  $\rho_s$ , the decrease in free-energy is computed by considering the free-energy changes along the isotherm 1-2-3-4-5 in Fig. 1 and works out to be

$$\Delta F_c = \rho_s \pi r^2 k_B T \ln\left(\frac{\rho_\infty}{\rho_i}\right) - \pi r^2 k_B T (\rho_\infty - \rho_s). \quad (4)$$

Here,  $\rho_\infty$  is the number density of the gas when it is in equilibrium with a straight interface at point 3 of the phase diagram and  $\rho_i \equiv N/V$  the initial number density of the vapor. The free-energy changes are computed by integrating the differential change in free energy at constant temperature,  $dF = -pdV$ . The first term represents the change in free energy along path 1-2-3 assuming that the supersaturated vapor behaves as an ideal gas and the second term represents the free-energy change along path 3-4. We have neglected the change in free energy of the solid when it is compressed to a high pressure along path 4-5. This is equivalent to assuming zero compressibility for the solid phase. In most physical situations even though the compressibility of the solid phase is not exactly zero, the slope of the isotherm on the  $P$ - $V$  curve is very high. Consequently the corresponding contribution to the free-energy change is small and the assumption that we make is therefore reasonable. We have also derived the Gibbs-Thomson formula with a nonzero compressibility for the solid by assuming that the vacancies in the solid behave as an ideal gas. However, we do not describe this here. The results from such an assumption produce an imperceptible change in the plots of the Gibbs-Thomson formula at the densities and temperatures of interest to us.

(c) A decrease in free energy of the noncondensing atoms as they expand to occupy the region left vacant by the condensing atoms,

$$\Delta F_{\text{nc}} = -(N - \rho_s \pi r^2) k_B T \ln\left(\frac{V - \pi r^2}{V - \rho_s \pi r^2 V/N}\right). \quad (5)$$

The total free-energy change is the sum of the above three pieces

$$\begin{aligned} \Delta F_{\text{tot}} = & 2\pi r\gamma + \rho_s \pi r^2 k_B T \ln\left(\frac{\rho_\infty}{\rho_i}\right) - \pi r^2 k_B T (\rho_\infty - \rho_s) \\ & - (N - \rho_s \pi r^2) k_B T \ln\left(\frac{V - \pi r^2}{V - \rho_s \pi r^2 V/N}\right). \end{aligned} \quad (6)$$

This is plotted for  $\rho_s = 0.996$ ,  $T = 1347$  K,  $\rho_\infty = 0.0036$ ,  $\gamma = 0.1173$ ,  $N = 120$ ,  $V = 10000$  in Fig. 2. This choice of numbers will become clear in Secs. III and IV, where we describe simulations performed with these parameters. It can be seen from Fig. 2 that the free energy has four extrema: a minimum ( $I$ ) at which an island is in true equilibrium with its surrounding vapor; a maximum ( $U$ ), at which a smaller island is in metastable equilibrium with the surrounding vapor; the unstable vapour phase itself ( $V$ ); and the unstable solid phase ( $S$ ). Extremizing the total free energy with respect to  $r$  yields

$$\ln\left(\frac{\rho_f}{\rho_\infty}\right) = \frac{\gamma}{r\rho_s k_B T} + \frac{\rho_f - \rho_\infty}{\rho_s}, \quad (7)$$

where  $\rho_f \equiv (N - \rho_s \pi r^2)/(V - \pi r^2)$  is the number density of the vapor surrounding the island. This form for the relationship between the radius of the island and the density of vapor surrounding it is true at both the maximum ( $U$ ) and the minimum ( $I$ ) and yields two roots for  $r$  at constant  $N$  and  $V$ , only one of which is stable. The second term on the right hand side of Eq. (7) is usually small<sup>6</sup> and is often neglected to yield a form for the density which is identical to Eq. (2).

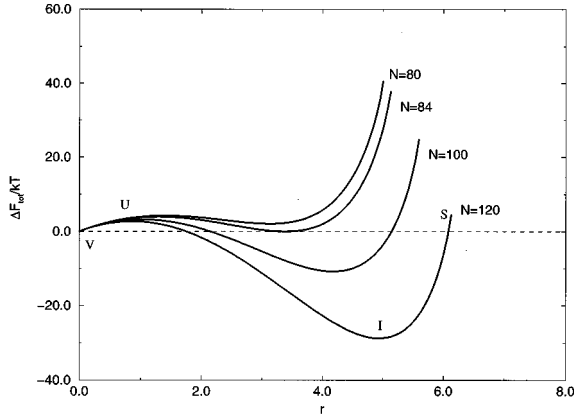


FIG. 2. The change in free energy as a function of  $r$ , for a system of volume  $V=10\,000$ , for various values of  $N$ . Notice the global minimum of the Helmholtz free energy is a solid island of radius  $r\sim 5$ , for the case  $N=120$ . Further, if  $N<84$ , the globally stable extremum switches from island plus vapor ( $I$ ) to pure vapor ( $V$ ).

This approximation is justified in our case too; a point we shall return to at the end of the next section.

### III. SIMULATION DETAILS

We perform Monte Carlo simulations of a lattice gas of “atoms” constrained to a single layer. The lattice gas Hamiltonian (for a square lattice in two dimensions) can be written as

$$\mathcal{H}_G = -\epsilon \sum_{\langle i,j \rangle} n_i n_j, \quad (8)$$

where  $n_i=1$  or  $0$  depending on whether site  $i$  is occupied by an atom. The sum runs over nearest neighbor ( $\langle i,j \rangle$ ) pairs and reduces the total energy by  $-\epsilon$  whenever two nearest neighbor sites are occupied. Thus,  $\epsilon$  represents a bond energy. We now briefly describe details of the simulation.

We use a continuous time Monte Carlo (MC) scheme<sup>9</sup> that helps reduce the time required to run the simulations. Barriers for moves of atoms in the MC were based on barriers for the Cu (100) surface calculated using effective medium theory.<sup>10</sup> They are allowed to depend on the coordination of the atom both before and after it makes a move. The barriers used are shown in Table I. The barriers are not all independent since they satisfy the constraint of detailed balance. Details regarding the choice of barriers as well as the number of barriers can be found in the paper referring to the

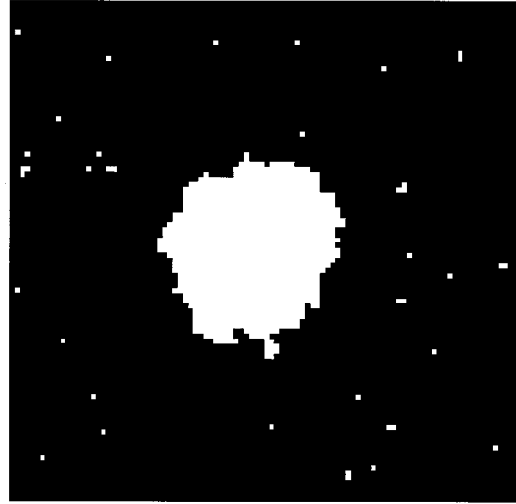


FIG. 3. A snapshot of an island with vapor around it as seen in the simulation.

decay of these islandlike features,<sup>3</sup> along with some other details regarding the simulation. The choice of barriers cannot affect the macroscopic static equilibrium behavior of the islands, but definitely plays a role in its dynamics. Macroscopic static behavior in equilibrium is governed solely by the bond energy. This is chosen to be  $\epsilon=0.341$  eV. For this bond energy, the critical temperature (at which all solid melts into gas) is  $T_c=2245$  K. This is known from the critical temperature of the Ising model to which this model can be mapped, as described later on in this section. Simulations were performed at temperatures of 1347 K and 1000 K, both well below the critical temperature. The system size was  $100\times 100$  lattice units and we ran the simulation by letting islands of different sizes come to equilibrium with their vapor. Time scales are governed by a global attempt frequency which was set to  $\nu=10^{12}$  s<sup>-1</sup>. The initial configuration in each run was a circular island, with no adatoms around it, sitting at the center of a vacant terrace, with periodic boundary conditions. The island would quickly source out atoms onto the terrace and come to equilibrium with this gas of atoms. The equilibrium between island and vapor is signaled by an island, the size of which fluctuates in time around a stable mean value. Figure 3 shows a snapshot of one of these islands in equilibrium with its vapor as seen in the simulation. Typically each of these runs made about 40–100 million MC moves and took about 4 to 9 h of CPU time on a IBM RS6000.

Once the island has come to equilibrium with its vapor

TABLE I. Energy barriers for intralayer atomic moves.

Initial coordination	Final coordination			
	zerofold	onefold	twofold	threefold
zerofold	0.697 eV	0.479 eV	0.328 eV	0.166 eV
onefold	0.820 eV	0.624 eV	0.450 eV	0.275 eV
twofold	1.010 eV	0.791 eV	0.591 eV	0.377 eV
threefold	1.189 eV	0.957 eV	0.718 eV	0.462 eV

one can compute its radius from a knowledge of its average size and one can also compute the average density of the gas around the island, by averaging at regular intervals of time, uncorrelated reports of the density. This is done for each of the islands of different initial size that we ran at the two temperatures mentioned above. There are various definitions possible for the radius of an island.<sup>6</sup> We compute its radius using the relation  $area = \pi r^2$ , where the area can be computed from the snapshots of the island that are reported (it includes the area of vacancies inside the island). The radius thus computed is equivalent to the equimolar radius  $r_e$  defined by Gibbs.<sup>6</sup> All length scales are measured in units of the lattice spacing which is set to 1.

The density of the gas is computed by counting the number of atoms on the terrace and then dividing this by the area of the terrace that is free for occupation by the gas. Care is taken to exclude a one-lattice spacing zone around the island as this cannot be occupied by an atom of the vapor (if it were it would be part of the island). In order to perform statistics we first compute the correlation time for the data. This is done by computing the autocorrelation of the island size as a function of time (in equilibrium). Typically, the autocorrelation decays with some time constant  $\tau$ . We then consider data points which are separated by more than a couple of time constants, as independent in time. Essentially, we bin the data into bins of size about  $2\tau$ , replacing the data with its average value in each bin. We then take an average of these average values and compute the standard deviation assuming the average data point in each bin to be uncorrelated with that in another bin. The same procedure is adopted to determine the density of gas around the island. This is how the error bars are obtained for plotting purposes.

Figure 4 shows a plot of the logarithm of the density of vapor versus the curvature ( $1/r$ ) of the island, for the two different temperatures. In order to compare the data to the prediction from the Gibbs-Thomson formula [Eq. (2)], we need the edge free energy  $\gamma$ , the density of the solid deep inside the bulk  $\rho_s$ , and the density of the vapor outside a straight interface  $\rho_\infty$ . These can be obtained by exploiting a mapping of the lattice gas to the Ising model, outlined below.

The Hamiltonian for the lattice gas [Eq. (8)] can be made to resemble that of an Ising model, using the transformation  $n_i = (1 + s_i)/2$ , to give

$$\mathcal{H}_I = -\epsilon/4 \sum_{\langle i,j \rangle} s_i s_j - \epsilon \sum_i s_i - N\epsilon/2, \quad (9)$$

where  $N$  is the total number of sites on the lattice and the spin  $s_i$  takes on values of  $\pm 1$ . The second term would be analogous to a field term in the Ising model with an external field of strength  $\epsilon$ .

This mapping helps us determine the parameters  $\gamma$ ,  $\rho_\infty$ , and  $\rho_s$ , that are relevant to this simulation. The edge free energy (i.e., surface tension),  $\gamma$ , is known as a function of temperature and orientation of the normal to the surface for the case of the two-dimensional Ising model.<sup>11</sup> It varies between a maximum and minimum value indicated in Table II and we see that the variation is not significant at the two temperatures at which we perform the simulations. We use an average value for the surface tension, which we approximate as

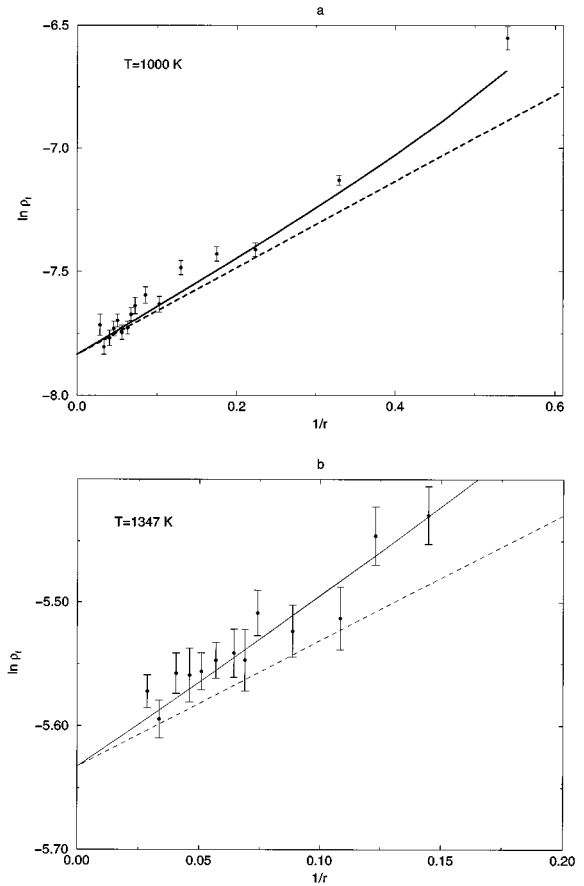


FIG. 4. Plot of the logarithm of the density of vapor outside an island vs the reciprocal of its equilibrium radius. The dashed line represents the Gibbs-Thomson prediction assuming an ideal gas of vapor. The solid curve is the prediction using the corrected Gibbs-Thomson formula for the Ising model. (a) is the data at a temperature of 1000 K, while (b) is at 1347 K.

$$\gamma_{\text{avg}} = \frac{\int \gamma ds}{\int ds} \approx \frac{\int \gamma^2 d\theta}{\int \gamma d\theta}. \quad (10)$$

The results of averaging are also indicated in Table II. Once again note that length scales are measured in terms of the lattice spacing which is set to 1. The values for  $\rho_\infty$  and  $\rho_s$  are known from the spontaneous magnetization. Using the mapping for lattice gas to Ising variables these can be calculated as  $\rho_\infty = (1 - m)/2$  and  $\rho_s = (1 + m)/2$ , where  $m$  is the spontaneous magnetization. The values of  $\rho_\infty$  and  $\rho_s$  are also indicated in Table II. Note that the density of the solid  $\rho_s$  is not identically equal to one. This is because of the presence of

TABLE II. Constants for the Ising model for bond energy = 0.341 eV.

	$T=1347$ K	$T=1000$ K
$T_c$	2245 K	2245 K
$\gamma_{\text{min}}$	0.1161 eV	0.1465 eV
$\gamma_{\text{max}}$	0.1184 eV	0.1543 eV
$\gamma_{\text{avg}}$	0.1173 eV	0.1507 eV
$\rho_\infty$	0.003578	0.000396
$\rho_s$	0.996422	0.999602

vacancies inside the solid, which can be seen even in the simulation. With this we have the three parameters necessary to plot the Gibbs-Thomson formula.

The dashed line in Fig. 4 is the ‘‘classical’’ Gibbs-Thomson prediction for the relationship between the density of vapor and radius of the island as defined in [Eq. (2)]. We see that the formula is satisfactory at large radii and low temperatures but important corrections are needed elsewhere. The next section discusses corrections to the ‘‘ideal-gas’’ equation of state used in the derivation of the Gibbs-Thomson formula.<sup>12</sup> Note that one may just fit the data to an exponential form given by the Gibbs-Thomson formula. This yields a value for the surface tension of  $1.59\gamma_{\text{avg}}$ . As one can see this is 60% off from the average value one would expect from the Ising model results. However, this is useful in fitting the data to an analytic expression of the Gibbs-Thomson form with a prefactor in the exponent, viz.,  $\rho \propto \exp[\alpha\gamma/(r\rho_s k_B T)]$ , where  $\alpha = 1.59$ .

#### IV. CORRECTED GIBBS-THOMSON FORMULA FOR THE ISING MODEL

The mapping from the lattice gas to the Ising model was discussed in Sec. III. This enables us to compute properties of the lattice gas system from a knowledge of the corresponding Ising system. We will be interested in obtaining corrections to the Gibbs-Thomson formula that take into account the ‘‘nonideal’’ nature of the gas of adatoms surrounding an island. To this end we rederive the Gibbs-Thomson formula using a more accurate equation of state than the ideal gas one for the lattice gas/Ising system, using high field series expansions.

One can obtain the Helmholtz free-energy per site of the Ising model (as a function of field, at a fixed temperature) by means of series expansions, starting from a very high value of the field. The first four terms of such an expansion of the equilibrium free energy for  $h > 0$  are

$$\begin{aligned} f^>[h] = & -h - \epsilon/2 - k_B t [\omega x^4 + \omega^2(2x^6 - 2.5x^8) \\ & + \omega^3(6x^8 - 16x^{10} + 31/3x^{12}) + \omega^4(x^8 + 18x^{10} - 85x^{12} \\ & + 118x^{14} - 209/4x^{16}) + \dots], \end{aligned} \quad (11)$$

where  $\omega \equiv \exp(-2h/(kT))$ ,  $x \equiv \exp(-\epsilon/(2k_B T))$ ,  $k_B$  is Boltzmann’s constant, and  $T$  the absolute temperature. The coefficients of various terms in this expansion are obtained analogous to low temperature expansions.<sup>13,14</sup> We use the first 13 terms of this expansion in our analysis. Differentiating the above expansion with respect to field yields an expansion for the magnetization per site as a function of field, for  $h > 0$ . The magnetization is odd in  $h$  (note the expansion is not),

$$\begin{aligned} m^>[h] = & 1 - 2[\omega x^4 + 2\omega^2(2x^6 - 2.5x^8) \\ & + 3\omega^3(6x^8 - 16x^{10} + 31/3x^{12}) + 4\omega^4(x^8 + 18x^{10} \\ & - 85x^{12} + 118x^{14} - 209/4x^{16}) + \dots]. \end{aligned} \quad (12)$$

The expressions for  $f[h]$  and  $m[h]$  for  $h < 0$  can be obtained by using the up-down symmetry of the Ising model. Thus,  $f^<[h] = f^>[-h]$  for  $h < 0$  and  $m^<[h] = -m^>[-h]$  for  $h < 0$ . This can be used to plot the equation of state for this

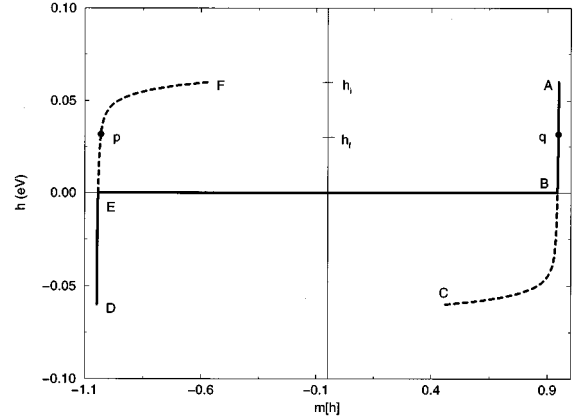


FIG. 5. Equation of state for the Ising model.

system (Fig. 5). For large positive values of the field, the state is essentially one in which all the spins are pointing up (or all  $n = 1$ , the solid phase). Conversely, the spins are all pointing down (gaseous phase of adatoms) for large negative values of the field. The dashed portions  $BC$  and  $EF$  on the equation of state represent metastable states and are analytic continuations of the equilibrium equation of state  $m[h]$ , i.e., we use  $m^>[h]$  as given by Eq. (12) for  $h < 0$  to generate the curve  $BC$ , on the equation of state. Note the similarity between this equation of state and the equation of state for an ideal gas (Fig. 1). Adatoms and solid can coexist in equilibrium at zero field. In this case, one has a flat interface between solid and gas. In addition to this one could have metastable states of the system wherein adatoms and solid coexist at a finite field (e.g., states  $p$  and  $q$  on the equation of state coexist at a field value of  $h_f$ ). However, in this case one could have a solid with a finite radius of curvature (just as in the ideal-gas case: points 5 and 2 in Fig. 1). In order to compute the radius of the solid in equilibrium with the gas of adatoms around it, one can compute the free-energy change in nucleating a solid, in a system of pure gas which is at state  $F$  on the phase diagram. The procedure adopted is similar to the one in Sec. II. However, one has to minimize the appropriate thermodynamic potential. For the ordinary Ising model (nonconserved order parameter) the Helmholtz free energy is at a minimum in the equilibrium state at constant temperature, volume, and external field. Since we work with a constant number of atoms in the lattice gas, the total magnetization of the Ising model is held fixed ( $M \equiv \sum_i s_i = \text{const}$ ). Consequently, one would have to minimize the Legendre transform of the Helmholtz free energy, which we shall henceforth refer to as the free energy,  $G(T, V, M) = F + Mh$  (it could also be called a thermodynamic potential). Consider starting out with a state consisting of  $N_i$  atoms uniformly distributed on a square lattice of volume  $V$  and having a magnetization corresponding to point  $F$  on the phase diagram. This state can lower its free energy by forming a solid island with vapor around it, the solid island being at point  $q$  of the phase diagram and the vapor at point  $p$ , at the same external field  $h_f$  as the solid. One can compute the change in the free energy in nucleating an island of up spins of radius  $r$  and this change is again composed of three pieces.

(a) An increase in surface free energy given by

$$\Delta G_{\text{edge}} = 2\pi r \gamma, \quad (13)$$

where  $\gamma$  is the line tension or edge free energy per unit length of the island.

(b) The change in free energy in the region of the island that condenses out. This change is computed by taking the difference in free energy between the initial state  $F$  and final state  $q$  and is given by

$$\Delta G_c = \pi r^2 (f^>[h_f] - f^<[h_i] + h_f m^>[h_f] - h_i m^<[h_i]). \quad (14)$$

(c) The change in free energy of the remaining region of volume  $(V - \pi r^2)$ , as it moves from point  $F$  of the metastable part of the phase diagram to point  $p$ ,

$$\Delta G_{nc} = (V - \pi r^2) (f^<[h_f] - f^<[h_i] + h_f m^<[h_f] - h_i m^<[h_i]). \quad (15)$$

The total change in free energy is thus

$$\begin{aligned} \Delta G_{tot} = & 2\pi r \gamma + \pi r^2 (f^>[h_f] - f^<[h_i] + h_f m^>[h_f] \\ & - h_i m^<[h_i]) + (V - \pi r^2) (f^<[h_f] - f^<[h_i] \\ & + h_f m^<[h_f] - h_i m^<[h_i]). \end{aligned} \quad (16)$$

Note that although the above equation for the free energy makes it look like a function of two independent variables,  $r$  and  $h_f$ , there is only one independent variable. The second variable is fixed by the constraint of conservation which can be expressed as

$$V m_i = \pi r^2 m^>[h_f] + (V - \pi r^2) m^<[h_f]. \quad (17)$$

Thus,  $\Delta G_{tot}$  can be looked upon as a function of  $r$  alone by replacing the final external field  $h_f$  that appears in Eq. (16) with the value obtained by formally solving for  $h_f$  as a function of  $r$  from Eq. (17). Extremizing Eq. (16) with respect to  $r$  yields the radius of the island in equilibrium with the gas. This gives us the analog of the Gibbs-Thomson formula for the lattice gas system,

$$\begin{aligned} \gamma + r (f^>[h] - f^<[h_f] + h_f (m^>[h_f] - m^<[h_f])) \\ + \frac{\partial h_f}{\partial r} \left( \frac{\pi r^2 h_f \chi^>[h_f] + (V - \pi r^2) h_f \chi^<[h_f]}{2\pi} \right) = 0, \end{aligned} \quad (18)$$

where  $\chi[h] \equiv \partial m / \partial h$  is the susceptibility and  $\partial h_f / \partial r$  can be determined from Eq. (17). Instead of regarding the above equation as an equation in  $r$ , we substitute for  $r$  in terms of  $h_f$  using the constraint [Eq. (17)]. This enables us to solve the above equation for  $h_f$  numerically after substituting the series expansions for the free energy, magnetization, and susceptibility. We use the first thirteen terms in the series expansion. On finding the equilibrium final external field  $h_f$ , for a given initial density of atoms, the equilibrium radius of the island at the extremum of the free energy can be obtained using the constraint [Eq. (17)]. The final field also tells us the final magnetization outside the island (point  $p$  on Fig. 5) and hence the density of adatoms outside  $\rho_f = (1 + m^<[h_f]) / 2$ . This gives us the required relation between the radius  $r$  of the island vs density of gas outside  $\rho_f$ , which we refer to as a corrected Gibbs-Thomson equation. The solid line in Fig. 4

represents the curve for the corrected Gibbs-Thomson formula. It is clearly seen that the corrected theory gives better agreement with the simulations than the continuum theory, particularly for islands of very small radii ( $r < 8$  or  $1/r > 0.125$ ). This leads us to believe that the approximation of an ideal gas of adatoms around the island is the principal cause for the break down of the classical Gibbs-Thomson formula at high vapor densities.

## V. STABILITY OF ISLANDS AND THE THERMODYNAMIC LIMIT

In this section we discuss the effects of finite size on the stability of the islands that we see in the simulation. We first look at finite size effects as predicted by the continuum version of the model that we have for a system of atoms (as in Sec. II). Figure 2 shows the effect of varying the number of atoms,  $N$ , at constant volume  $V$ , on the total free-energy change in nucleating an island. We see that the stable minimum ( $I$ ) is no longer a global minimum of the free-energy of the system once  $N$  falls below a certain value and later this minimum vanishes completely (the curve becomes flat) below a certain critical value of  $N$  which we denote as  $N_{cr}(V)$ , which evidently depends on  $V$ . Similar behavior is observed if we increase the volume  $V$  at constant  $N$ . However, if we take the thermodynamic limit at constant initial density ( $\rho_i = \text{const}$ ,  $V \rightarrow \infty$ ) the stable minimum persists and moves off towards  $r = \infty$ . These results can be understood by means of a stability analysis.

The equilibrium between an island and the vapor around it is dynamic in nature and can be understood as a balance between the rate at which atoms from the vapor attach themselves to the perimeter of the island and the rate at which atoms detach themselves from the perimeter of the island to become part of the vapor. The former rate would be proportional to the density of the vapor surrounding the island, while the latter would be governed purely by temperature and would be independent of the density of vapor surrounding the island, in the low density limit.

Consider a change in the radius of an island in equilibrium with its vapor. If the island grows from an initial radius  $r$  to a radius  $r + dr$  by swallowing some atoms from the vapor phase, the concomitant change in the density of the vapor would be

$$d\rho_f = - \frac{2\pi r (\rho_s - \rho_f) dr}{V - \pi r^2}. \quad (19)$$

If the new island of radius  $r + dr$  is to be in equilibrium with vapor around it, one can compute the change in equilibrium vapor density around it (i.e., the difference between the vapor density around an island of radius  $r + dr$  and the vapor density around an island of radius  $r$ ) from the Gibbs-Thomson formula [Eq. (7)],

$$d\rho_f = - \frac{\gamma \rho_f dr}{k_B T r^2 (\rho_s - \rho_f)}. \quad (20)$$

The above two equations predict that the density will decrease if the island grows ( $dr > 0$ ), which is to be expected. If the actual change in density [Eq. (19)] is larger in magnitude (smaller in value) than that dictated by equilibrium [Eq.

(20)] the island would be stable. This is because the new density around the island is too low and consequently the new attachment rate would be lower than the detachment rate. This in turn would force more atoms to detach from the island, thus bringing down the size of the island. From this one can conclude that for stability one needs

$$-\frac{2\pi r(\rho_s - \rho_f)dr}{V - \pi r^2} < -\frac{\gamma \rho_f dr}{k_B T r^2 (\rho_s - \rho_f)}, \quad (21)$$

which can be written as

$$r^3 > \frac{\gamma \rho_i V}{2\pi k_B T (\rho_s - \rho_i)^2} \left(1 - \frac{\pi r^2}{V}\right)^2 \left(1 - \frac{\rho_s \pi r^2}{\rho_i V}\right), \quad (22)$$

where  $\rho_i = N/V$  as before. We see from this that for stability the radius of an island should be greater than a certain minimum value which is obtained by solving

$$r_{\min} = \left(\frac{\gamma \rho_i V}{2\pi k_B T (\rho_s - \rho_i)^2}\right)^{1/3} \left(1 - \frac{\pi r_{\min}^2}{V}\right)^{2/3} \left(1 - \frac{\rho_s \pi r_{\min}^2}{\rho_i V}\right)^{1/3}. \quad (23)$$

Along with this if we use the Gibbs-Thomson formula [Eq. (2)] we can obtain a relation for the critical value  $N_{\text{cr}}$  as a function of the volume. All issues of local stability of the islands can be resolved using these equations. The curve  $N_{\text{cr}}(V)$  in  $N-V$  space defines a boundary between regions where one can have stable islands and regions where one can have no stable islands.<sup>15</sup>

One can show that for large system size the last two terms in the product of Eq. (23) go to unity and we have

$$r_{\min}^3 = \gamma \rho_i V / [2\pi k_B T (\rho_s - \rho_i)^2]. \quad (24)$$

This shows that the minimum radius of a stable island grows as the one third power of the volume of the box in two dimensions.

We now digress to note the behavior of the unstable root ( $U$ ) of the free energy in Fig. 2 in the thermodynamic limit. It is seen that the unstable root does not scale with system size by plotting this root obtained by numerical solutions versus the system volume  $V$ . The unstable root reaches a limiting value in the limit  $V \rightarrow \infty$ , which can be obtained from Eq. (7) by neglecting terms of order  $r^2/V$ . The critical radius  $r^*$ , which is obtained by taking this limit, is given by

$$r^* = \frac{\gamma}{k_B T [\rho_s \ln(\rho_i / \rho_\infty) + (\rho_\infty - \rho_i)]}. \quad (25)$$

This form is identical to the form for the critical radius quoted in the context of nucleation theory.<sup>5</sup> The nucleation barrier, which is the free-energy barrier that the system of supersaturated vapor should overcome in order to form a stable island plus vapor, attains a limiting value of

$$\Delta F^* = \frac{\pi \gamma^2 [\rho_s \ln(\rho_i / \rho_\infty) + \rho_\infty + \rho_s - 2\rho_i]}{k_B T [\rho_s \ln(\rho_i / \rho_\infty) + \rho_\infty - \rho_i]^2}. \quad (26)$$

How about seeing the unstable islands in our simulation? We have observed that if we start out with 109 atoms in a

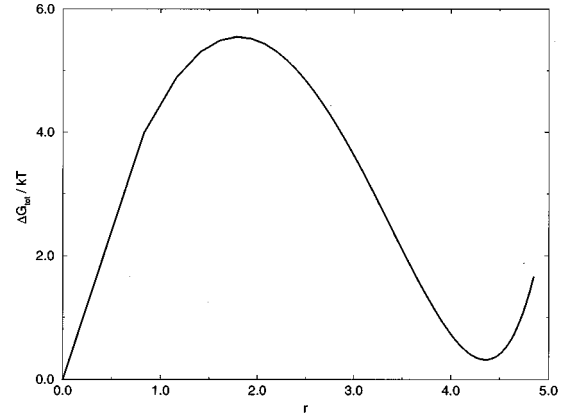


FIG. 6. The free energy of an island of radius  $r$  plotted for a system of 109 particles with  $V = 10\,000$ .

$100 \times 100$  system at a temperature of 1347 K, the island size fluctuates considerably and there are several frames of data where the island breaks up into many smaller ones. This can be understood within the framework of our theory for the Ising model. Figure 6 shows the change in free energy on nucleating an island of radius  $r$  in the Ising model for 109 particles. From this we see that the island-vapor system is not a point of global minimum of free energy. Further the nucleation barrier to go from this state to one of uniform vapor is given by  $\Delta G/k_B T = 5.26$ . Also, we can see from this figure that the fluctuations to various other island sizes are not highly unlikely. This would account for the large fluctuations in island size. The same effect is seen for 25 particles at a temperature of 1000 K.

## VI. INVESTIGATION OF MICROSCOPIC ORIGINS

Since these simulations of atomic scale systems exhibit the Gibbs-Thomson effect, viz., an enhanced vapor pressure around islands of small radii relative to the vapor pressure outside a flat interface, the opportunity arises to investigate the relationship between this thermodynamic effect and the microscopic dynamics. We may ask, from a microscopic point of view, what is the origin of the enhanced adatom vapor concentration in equilibrium with a small island. A complete discussion of this issue involves many details of the microscopic characteristics of the island-vapor interface, which are beyond the scope of this paper. Here we outline our main findings; the interested reader is referred to Refs. 16 and 17 for further details.

As discussed in Sec. V, equilibrium between the island and vapor implies detailed balance at the interface: atoms are attaching to and detaching from the island with equal rates. Analysis of our simulations shows that for small equilibrium islands, the interface transfer activity is enhanced in proportion to the vapor density. For example, the data points in Fig. 7 show the rate at which atoms detach from an island per unit length of the macroscopic island-vapor interface. This leads to the following microscopic interpretation of the Gibbs-Thomson effect. As the island size decreases, it becomes easier for atoms to detach from it, raising the detachment current density. However, we find that there is no noticeable change in the ease with which an atom can attach to

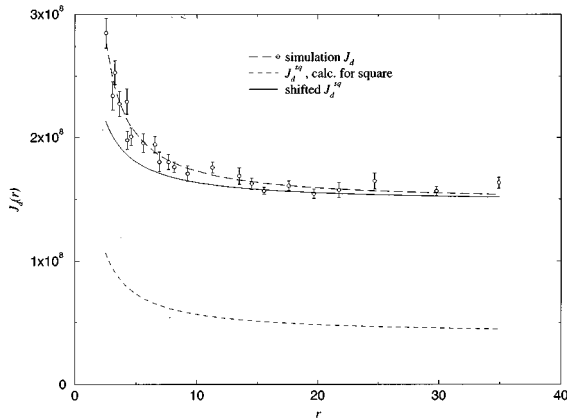


FIG. 7. A comparison of the changes in detachment current density found for islands in simulation ( $J_d$ ), and for a square island treated in the same way ( $J_d^{\text{sq}}$ ). The solid line represents  $J_d^{\text{sq}} + A$ , where  $A$  is chosen such that  $J_d - (J_d^{\text{sq}} + A) \rightarrow 0$  as  $r \rightarrow \infty$ . Lines, to guide the eye, are fits to the form  $f(\infty)\exp(C/r)$ .

the island for islands, the radii of which vary between 4 and 35. Therefore, a higher vapor density is required to maintain dynamic equilibrium.

The enhanced detachment current density for smaller islands can be ascribed to trends in the character of the sites on the island edge. On smaller islands, the density of edge atoms is found to actually decrease, so that there are fewer atoms per unit length of interface available for detachment. However, the average coordination of the edge atoms is found to be smaller, which leads to lower energy barriers for edge atom motion. Also, each edge atom on a smaller island tends to have more detachment moves available to it. That is, when the edge atom moves it is more likely to detach, as opposed to moving along the edge of the island. The net result of these trends yields the observed enhancement in detachment.

Note that the above trends, observed in the equilibrium islands (e.g., Fig. 3) of our simulations also hold true for a square island, although a square is not the thermodynamic shape of an equilibrium island at finite temperatures. As a square island is made smaller, the corner sites acquire greater significance. Since the corner sites of a square island have a lower coordination than sites on the side of a square, the average coordination of edge atoms on a small square is lower than it is on a large square. Similarly, corner atoms have two detachment moves available, while side atoms have only one. Therefore, a smaller square has a higher ratio of available detachment moves to number of edge atoms.

This analogy between the simulated islands and square islands suggests that an important element of the observed behavior is the simple geometric constraint that any closed perimeter on a square lattice must have four more outward pointing corners than it has inward pointing crevices. As a test of this idea, Fig. 7 compares the detachment current density observed in the simulation with that expected for a square island of the same area and at the same temperature. As expected, the overall detachment current density is lower for the square island, as it has the smoother edge. However, as the island size is varied, the magnitude of the enhancement in detachment from the square is comparable to the

enhancement in detachment from the simulated islands. It is, therefore, clear that it is important to consider the effect of the ‘‘four extra corners’’ in an understanding of the Gibbs-Thomson effect at a microscopic level. It is difficult to quantify the effect of this geometrical constraint, as it is impossible to label an individual corner on an equilibrium island as being due to either geometry or thermal roughening. However, comparison with the nonequilibrium square island gives an indication of the strength of the effect.

## VII. CONCLUSIONS

We have simulated a lattice gas to mimic the behavior of a cluster of atoms, on generic surfaces, in an effort to study the relationship between the cluster radius and the vapor density around it. We have shown that the ‘‘classical’’ Gibbs-Thomson relationship one computes assuming an ideal gas of atoms is incorrect at high vapor densities and a knowledge of the true equation of state is necessary to obtain a better result. We have seen that the corrected formula can be used down to islands with about 150 atoms at a temperature of  $0.6 T_c$  and islands with about 30 atoms at  $0.445 T_c$ , in the case of our simulations.

Further, we have seen how metastable states in traditional nucleation theories can be made stable by finite size effects. We have seen how these states may arise in the context of the Ising model and have explored the metastable continuation of the equation of state in the Ising model. Simulations performed on the Ising model agree well with our predictions regarding stability.

As far as experimental observations of the corrections to the Gibbs-Thomson formula are concerned, such an effect would surely be observed in a system with short range interactions at small island sizes and high temperature (about 60% of the melting temperature). However, in real situations in addition to the short range attractive forces that bind atoms to each other there exist long range dipolar forces at step edges, between the atoms at the edge and the vapor. This may skew the predictions of a theory like ours which is simple and ignores such effects. Finally, we have looked at the microscopic origins of the Gibbs-Thomson formula and have offered heuristic arguments that it maybe correlated to geometric constraints.

## ACKNOWLEDGMENTS

B.K. would like to thank Gerard Barkema for helping out with a lot of information regarding the MC method and for the data on energy barriers for which we are grateful to Rien Breeman. He would also like to thank Mark Newman for help on series expansions. We would like to thank Eric Chason for a lot of help on details regarding the simulation. B.K. wishes to acknowledge financial support from the National Science Foundation and the Materials Science Centre through Grant Nos. NSF-GER-9022961 and DMR-91-

21654, respectively, while J.M. acknowledges support from the Air Force Office of Sponsored Research (Grants Nos. AFOSR-91-0137 and AFOSR/AASERT F49620-93-1-0504) and partial support from the Cornell Materials Science Cen-

tre (NSF-DMR-91-21654). This work made use of the MSC Multi-User-Computer Facility, an MRL Central Facility supported by the National Science Foundation under Award No. DMR-9121564.

\*Present Address: Dept. of Chemistry, UCSD, La Jolla, CA 92093-0358.

<sup>1</sup>G. W. Greenwood, *Acta Metall.* **4**, 243 (1956); I. M. Lifshitz and V. V. Slezov, *Zh. Éksp. Teor. Fiz.* **35**, 479 (1958) [*Sov. Phys. JETP* **8**, 331 (1959)]; I. M. Lifshitz and V. V. Slezov, *J. Phys. Chem. Solids*, **19**, 35 (1961); C. Wagner, *Z. Elektrochem.* **65**, 581 (1961); B. K. Chakraverty, *J. Phys. Chem. Solids* **28**, 2401 (1967).

<sup>2</sup>D. R. Peale and B. H. Cooper, *J. Vac. Sci. Technol. A* **10**, 2210 (1992).

<sup>3</sup>J. G. McLean, J. P. Sethna, B. Krishnamachari, B. H. Cooper, D. R. Peale, and E. Chason (unpublished).

<sup>4</sup>K. Morgenstern, G. Rosenfeld and G. Comsa, *Phys. Rev. Lett.* **76**, 2113 (1996).

<sup>5</sup>J. E. McDonald, *Am. J. Phys.* **30**, 870 (1962).

<sup>6</sup>J. S. Rowlinson and B. Widom, *Molecular Theory of Capillarity* (Clarendon Press, Oxford, 1982), Chap. 2, pp. 25–47.

<sup>7</sup>O. H. Nielsen, J. P. Sethna, P. Stoltze, K. W. Jacobsen, and J. K. Nørskov, *Europhys. Lett.* **26**, 51 (1994).

<sup>8</sup>Note that the solid island (point 5) is not at the same pressure as the vapor in equilibrium around it (point 2) if the island has a finite radius of curvature. The difference in pressure between the solid and gas is given by the Young-Laplace equation in two dimensions,  $\Delta p = \gamma/r$ , where  $\gamma$  is the edge free energy and  $r$  the radius of curvature of the island.

<sup>9</sup>A. B. Bortz, M. H. Kalos, and J. L. Lebowitz, *J. Comp. Phys.* **17**, 10 (1975).

<sup>10</sup>M. Breeman, G. T. Barkema, and D. O. Boerma, *Surf. Sci.* **303**, 25 (1994).

<sup>11</sup>J. E. Avron, H. Van Beijeren, L. S. Schulman, and R. K. P. Zia, *J. Phys. A* **15**, L81 (1982).

<sup>12</sup>One may suspect the assumption of zero compressibility for the solid phase may be the reason for the discrepancy between the data and the fit using the Gibbs-Thomson formula, as opposed to “nonideal” behavior of the gas around the island. However, this is ruled out because we have rederived the Gibbs-Thomson formula, assuming the vacancies in the solid phase to behave as an ideal gas. The curve so obtained is virtually indistinguishable from the dotted curve in Fig. 4 which represents the classical uncorrected Gibbs-Thomson formula. The inclusion of the extra term on the right hand side of Eq. (7) does not produce any discernable change either to the classical uncorrected Gibbs-Thomson curve.

<sup>13</sup>G. Parisi, *Statistical Field Theory* (Addison-Wesley, New York, 1988), Chap. 4, pp. 46–49.

<sup>14</sup>M. F. Sykes, J. W. Essam, and D. S. Gaunt, *J. Math. Phys.* **6**, 283 (1965).

<sup>15</sup>An alternate route to obtaining these relations would be to make sure that we are at a local minimum of the total change in free energy that we derived in Sec. II, Eq. (6), i.e.,

$$\frac{d\Delta F_{\text{tot}}}{dr} = 0,$$

$$\frac{d^2\Delta F_{\text{tot}}}{dr^2} \geq 0.$$

The first of the above two equations is just the Gibbs-Thomson formula as we have seen in Sec. II, while the second one which expresses the fact that we are at a local minimum of the free energy, reduces to Eq. (22).

<sup>16</sup>J. G. McLean, Ph.D. thesis, Cornell University, 1996.

<sup>17</sup>J. G. Mclean, J. P. Sethna, and B. H. Cooper (unpublished).